Defence Science Journal, Vol. 58, No. 2, March 2008, pp. 275-284

Dynamic Yield Strength of Mild Steel under Impact Loading

Manjit Singh, D. Sood, R.K. Gupta, R. Kumar, P.C. Gautam, Bhupinder Sewak, A.C. Sharma, and Thomson Mathew

Terminal Ballistics Research Laboratory, Sector-30, Chandigarh

ABSTRACT

Dynamic yield strength of mild steel is estimated when impacted by the steel balls launched by two stage-light gas gun in the velocity region 1900-5200 m/s. The ball impact provides a radial momentum to the target material resulting in a crater which spreads out until it is stopped by the target yield strength. The dynamic yield strength of target metal is calculated by incorporating the densities of ball and target material along with experimentally measured crater radius and impact velocity in modified Bernoulli's equation. The dynamic yield strength of mild steel has been found to be around 2000 MPa under high velocity impact, causing the material to deform at strain rates > 10^6 s^{-1}. Impact phenomenon was also simulated on Autodyn 2-D using Euler processor. Simulation results reveal that the target material is subjected to the highest strain rate of 10^5 - 10^6 s^{-1} at the impact point and then decreases as the penetration progresses through the target. Predicted results of crater radius depth, and splash of material match with the experimental measurements.

Keywords: Ball impact, gas gun, flash ray, crater growth, strain rate, dynamic yield strength, autodyn simulation, strength model, Eulerian solver, Johnson & Cook strength model

NOMENCLATURE

A_o	Cross-sectional area of projectile
A	Cross-sectional area of crater
P	Stagnation pressure
P_o	Initial pressure
r_c	Crater radius
r_p	Projectile radius
r_{cm}	Maximum crater radius
U	Penetration velocity
u_c	Crater expansion velocity
V_p	Projectile velocity
ρ_p	Projectile density
ρ_t	Target density
σ_p	Projectile yield strength
σ_t	Target yield strength
σ	Flow stress
ε	Strain
$\dot{\gamma}$	Strain rate
L_p	Length of projectile

Received 31 October 2007

1. INTRODUCTION

The strength properties of materials at high strain rate are needed in determining the response of structures to the dynamic loading, associated with the shock and impact loading processes. It is well known that the yield strength and the ultimate tensile strength of materials are determined by the behaviour of dislocations, and these depend on both the pre-history of loading and strain rate. For FCC metals, at low strain rates, the true stress increases linearly with the logarithm of strain rate. At high strain rates exceeding 10^3 s^{-1}, the true stress increases approximately linearly with the strain rate. These experimental observations have been explained on the basis of transitions in the rate controlling deformation mechanism with increasing strain rates[1]. At low strain rates, thermal activation is required to assist a dislocation to cross the barriers. However, at the high strain rates, the continuous motion of dislocation moving through a lattice is resisted by lattice potential itself, as well as by the interactions with the phonons, electrons, and radiations. These dissipative processes are viscous in nature and lead to a linear dependence of flow stress on the applied strain rate. Therefore, with the increase in strain rate, plastic flow of metal changes from a thermal activation to the one with viscous drag. The variation of flow stress with strain rate at different temperature for FCC metals is shown in Fig. 1.

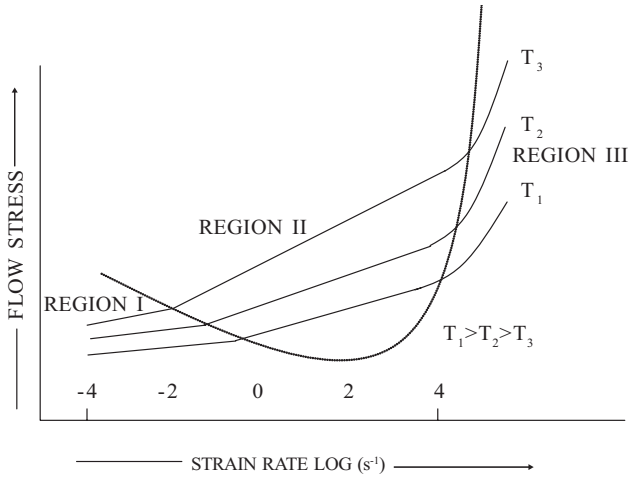

Figure 1. Variation of the flow stress of FCC metals with strain rate at different temperatures.

The dynamic tensile strength of a metallic material depends upon the strain, strain rate, temperature, and sometime on the crystal structure also. The dependence of dynamic flow stress on these parameters can be expressed through the mechanical equation of state written as

$$d\sigma = \left(\frac{\partial \sigma}{\partial \varepsilon}\right)_{\dot{\varepsilon},T} d\varepsilon + \left(\frac{\partial \sigma}{\partial \dot{\varepsilon}}\right)_{\varepsilon,T} d\dot{\varepsilon} + \left(\frac{\partial \sigma}{\partial T}\right)_{\varepsilon,\dot{\varepsilon}} dT \quad (1)$$

where the first term on the right hand side is strain hardening, the second term is strain rate sensitivity, and the third term is thermal softening. The first two terms are positive in the sense that flow stress increases with increase in the strain and strain rate, whereas the third term is negative because the flow stress of the material decreases at elevated temperatures.

There are different ways of estimating the dynamic tensile strength of metals. The rupture strength of metals at high strain rates has been determined from the measurements of length and velocity[2, 3] of the different particles of the stretching and particulating metal jets. The phenomena of shaped charge liner collapse and shock-induced cavity collapse have been used for subjecting the metal to high strain rates in the form of jets. The dynamic yield strength of target metal can be calculated[4] from the growth of the crater formed by the impact of a high velocity projectile on to the target. From the measurements of ratio of crater to impact or radius, impact velocity along with the densities of impactor and target metals, the dynamic yield strength of the metals has been calculated.

In the present studies, ball impact experiments have been performed using the two-stage light gas gun facility at Terminal Ballistics Research Laboratory (TBRL), Chandigarh. The dynamic yield strength of mild steel is estimated by solving crater growth equation along with experimentally measured impact velocity and crater radius.

2. CRATER GROWTH UNDER PROJECTILE IMPACT

Consider a projectile of velocity V_p and density r_p, penetrating at a speed U in a semi-infinite

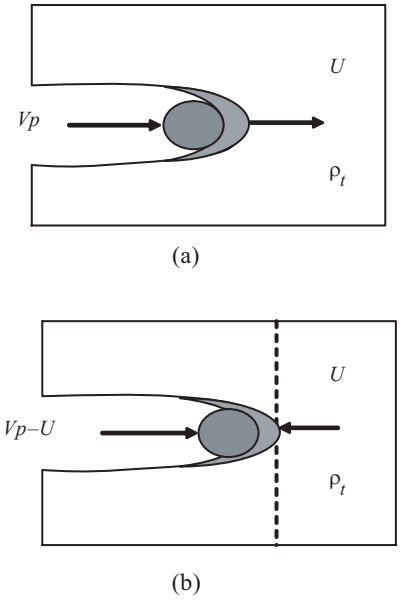

Figure 2: Process of projectile penetration in target material of density r_t in: (a) stationary and (b) moving coordinate system.

target material of density r_t. The process of projectile penetration in the target material is shown in Fig 2. In the coordinate system moving with velocity U [Fig 2(b)], the projectile moves to the right with velocity $V_p - U$ and the target moves to the left with velocity U. If we assume that the yield strengths of projectile and target materials are small in comparison to impact pressure of projectile, the flow can be treated as fluid. The pressure on the two sides of the surface moving to the right with penetration velocity U, must be the same. By using Bernoulli's theorem:

$$\frac{1}{2}\rho_p\left(V_p - U\right)^2 = \frac{1}{2}\rho_t U^2 \tag{2}$$

The total hydrodynamic penetration is given by

$$L_p = Ut_p = \frac{UL}{V_p - U} \tag{3}$$

where, t is the time of penetration and L is the length of the jet. Eliminating V and U from Eqns (2) and (3), the total penetration length can be written as

$$L_p = L\sqrt{\left(\frac{\rho_p}{\rho_t}\right)} \tag{4}$$

However, if the target and projectile strengths are comparable with impact pressure, Eqn (2) is modified[5] as

$$\sigma_p + \frac{1}{2}\rho_p\left[V_p - U\right]^2 = \sigma_t + \frac{1}{2}\rho_t U^2 \tag{5}$$

where σ_p and σ_t are the yield strengths of projectile and target materials, respectively. The difference (σ_t, σ_p) can be calculated by measuring the projectile and penetration velocities, simultaneously. Thus the target strength obtained from Eqn (5) will be the target strength to resist penetration. This is nearly a continuous high strain rate process. However, the target strength determined from the measurements of crater radius gives unsteady inertial radial flow of the target material.

The radial velocity u_c, which is initially equal to the crater expansion velocity U, decreases to zero as the crater radius increases to its maximum value. The projectile material flows out of the interaction region due to relative velocity V-U. Here, it is assumed that the eroded material flows only radially and exerts a pressure P on the expanding crater wall. This imparts a velocity u_c to the crater wall, against the constant resistive pressure σ_t due to target strength. The velocity components in the crater formation by projectile are shown in Fig. 3. The initial pressure P_o is assumed to be the steady state hydrodynamic pressure, which equals to rate of transfer of momentum in a unit area of target. It is given by the relation

$$P_o = \frac{1}{2}\rho_p\left(V_p - u_c\right)^2 \tag{6}$$

The crater velocity U, which is assumed to be equal to the crater expansion radial velocity u_c can be written from Eqn (2) as

$$U = u_c = \frac{V_p}{1 + \sqrt{\rho_t / \rho_p}} \tag{7}$$

where ρ_t and ρ_p are the target and projectile material densities, respectively.

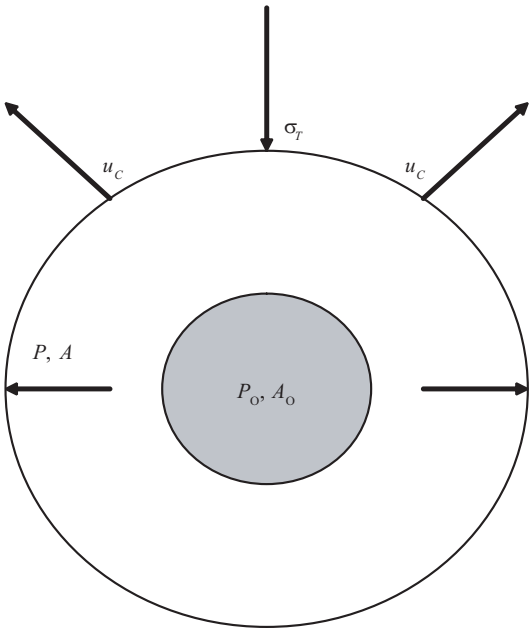

Figure 3. Expansion of a crater under pressure *P* due to projectile penetration in the target.

Substituting u_c in Eqn (6), the initial pressure can be written as

$$P_0 = \frac{\rho_t V_p^2}{2\left(1+\sqrt{\frac{\rho_t}{\rho_p}}\right)^2} \tag{8}$$

The stagnation pressure P acting on the crater wall decreases with increasing crater area A, as

$$P = \frac{P_0 A_0}{A} \tag{9}$$

The stagnation pressure P, according to Bernoulli's equation, is related to the crater velocity u_c and the material strength[6] as

$$P = \frac{1}{2}\rho_t u_c^2 + \sigma_t \tag{10}$$

Eliminating P from the Eqns (9) and (10) gives

$$u_c = \frac{dr_c}{dt} = \left(\frac{2P_0 A_0}{\rho_t A} - \frac{2\sigma_t}{\rho_t}\right)^{1/2} \tag{11}$$

The area ratio A_0/A can be replaced by r_p^2/r_c^2, to give

$$\frac{dr_c}{dt} = \left(\frac{2P_0 r_p^2}{\rho_t r_c^2} - \frac{2\sigma_t}{\rho_t}\right)^{1/2} \text{ or } dt = \frac{dr_c}{\sqrt{\frac{A}{r_c^2} - B}} \tag{12}$$

where

$$A = \frac{2r_p^2 P_o}{\rho_t} = \frac{r_j^2 V_p^2}{\left(1+\sqrt{\frac{\rho_t}{\rho_p}}\right)^2} = r_p^2 u_C^2 \quad \text{and}$$

$$B = \frac{2\sigma_t}{\rho_t} \tag{13}$$

Integrating the Eqn (12) between the limits $t = 0$ for $r_c = r_p$ and $t = t$ for $r_c = r_c$, gives

$$t = \frac{1}{\sqrt{B}}\left[\sqrt{\left(A/B - r_p^2\right)} - \sqrt{A/B - r_c^2}\right] \tag{14}$$

Equation (14) gives the growth of crater with time. The crater will no longer grow when $r_c^2 = A/B$. Thus, the maximum crater radius can be written as

$$r_{cm} = \sqrt{A/B} \tag{15}$$

Putting the values of A and B from Eqn (13) gives

$$r_{cm} = \sqrt{\frac{r_p^2 V_p^2 \rho_t}{2\sigma_t\left(1+\sqrt{\rho_t/\rho_p}\right)^2}} \tag{16}$$

This equation can be rearranged to give target yield strength as

$$\sigma_t = \frac{r_p^2 V_p^2 \rho_t}{2r_{cm}^2\left(1+\sqrt{\rho_t/\rho_p}\right)^2} \tag{17}$$

Thus, the target yield strength σ_t can be calculated from the known projectile velocity V_p, projectile

Table 1. Classification of strain rate studies in different regions and different methods of loading

Region	Creep	Static	Intermediate	High	Very high
Time scale (s)	10^{6} -10^{4}	10^{2} - 10^{1}	10^{0} - 10^{-1}	10^{-2} - 10^{-4}	10^{-6} - 10^{-8}
Strain rate (s)	10^{-8} -10^{-6}	10^{-6} - 10^{-3}	10^{-3} – 10^{0}	10^{0} - 10^{4}	10^{4} - 10^{8}
Methods of loading	Stress machine	Screw or hydraulic machine	Mechanical machine	Taylor impact cylinder expansion Hopkinson pressure bar	Plate/ball impact Shock loading
Dynamic considerations	Inertial forces neglected isothermal process			Inertial forces important adiabatic process	
	No wave propagation	Elastic and plastic waves propagation		Shock waves propagation	

radius r_p, crater radius r_{cm}, and the projectile and target densities.

3. IMPACT EXPERIMENTS

Mechanical properties of the materials are studied in different regions of strain rates using different experimental techniques, as given in Table 1. In low to intermediate strain rates, different types of mechanical machines are used. For high strain rates studies, Taylor Impact Test, Split Hopkinson Pressure Bar (SHPB), and Plate Impact Tests are used. Taylor Impact Test is a simple test for determining the dynamic yield strength of metals. In the original experiments by Taylor[7], the specimens were impacted at a high velocity against a rigid anvil. The impact resulted in mushroom shaped deformed specimens.

Using the measurements of the undeformed and deformed shapes along with the impact velocity, the dynamic yield strength was calculated. The results for copper and iron cylinder[8] in Taylor test were used to derive the constitutive equation of materials at high strain rate. The SHPB method[9,10] has been used successfully for loading the material, up to the strain rate of 10^{4} s^{-1}. For obtaining the strain rates > 10^{4} s^{-1}, shock loading of the material by explosive detonation or projectile impact is required. For very high strain rates, 10^{5}-10^{8} s^{-1} plate impact[11] experiments have been used.

Impact experiments for the present studies were performed using two-stage light gas gun facility at TBRL. The steel balls SS-4340 of dia 7 to 15 mm and mass up to 8 g were launched to velocities 1900 – 5200 m/s using 29 mm and 40 mm caliber launch tubes. A steel ball was placed inside a polycarbonate sabot of outer dia matching with the launch tube caliber. The weights of propellant,

Figure 4(a). Two-stage light gas gun facility at TBRL.

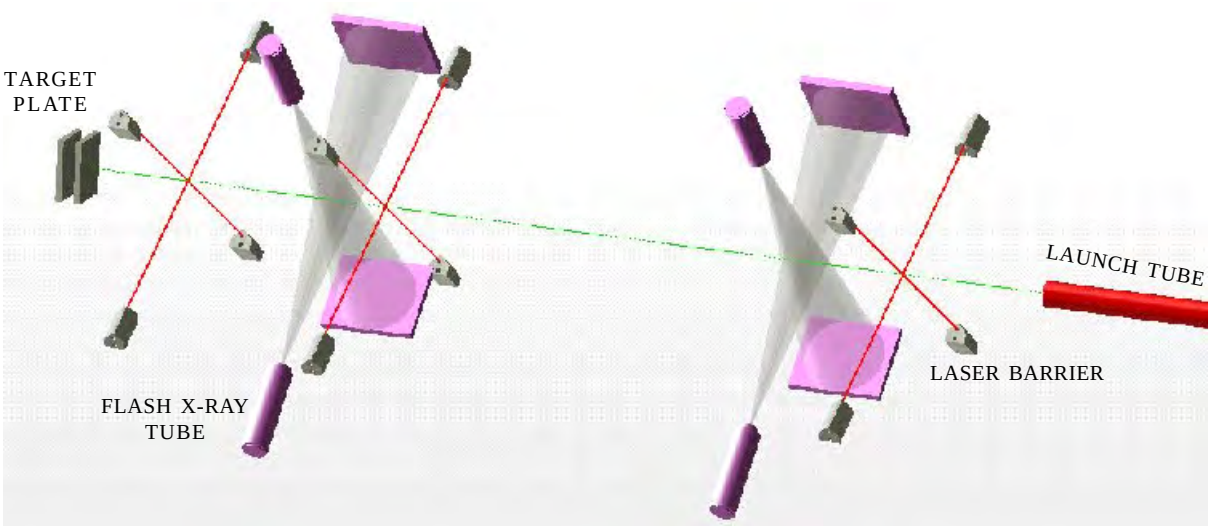

Figure 4(b). Layout for ball impact experiments.

piston, initial hydrogen pressure in the pump tube, and rupture disc thickness were optimised using CESAR internal ballistics software to achieve the desired velocity. The projectile velocity before impact was measured using laser barrier velocity measurement system. Sabot separation and impact process were radiographed using four channels of 150 KV flash x-ray system. A view of the gas gun facility and experimental layout used for conducting ball impact experiments is shown in Figs 4(a) and 4(b).

In all the experiments, single or air-spaced, mild steel plates of size 250×250×32 mm were used as target assembly. The targets were placed at 8 m from the muzzle end of the launch tube and vacuum of 150 mbar was maintained ahead of the projectile. The steel ball in flight along with the polycarbonate sabot and the splash of target material on impact with the ball as captured by flash x-ray system are shown in Figs 5(a) and 5(b).

4. SIMULATION OF IMPACT PHENOMENON

Impact phenomenon was simulated using Autodyn 2-D software using Eulerian solver. Few cycles selected from the animation of the impact of a 10 mm dia steel ball impacting mild steel plate at velocity 1888 m/s is shown in Fig. 6. Johnson and Cook strength model and Hydro min. failure model were selected for the target material. The crater

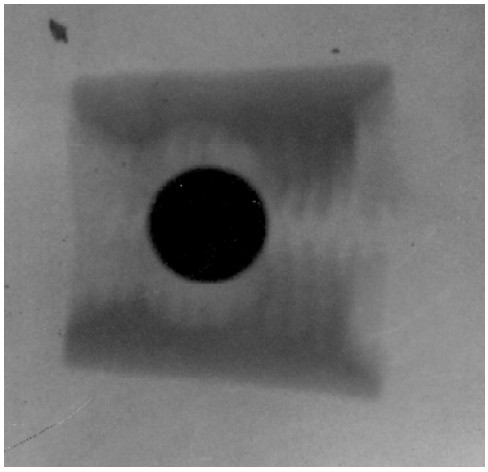

(a)

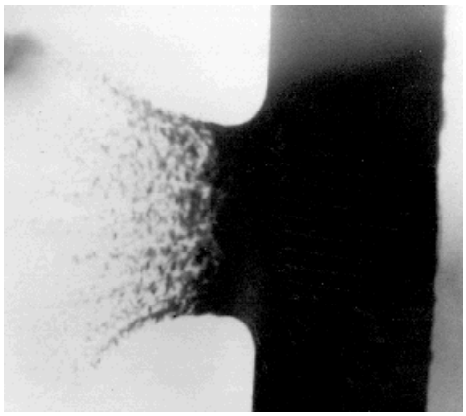

(b)

Figure 5. Flash x-ray images of: (a) sabot separation of steel ball in flight and (b) splash of target material due to impact of steel ball.

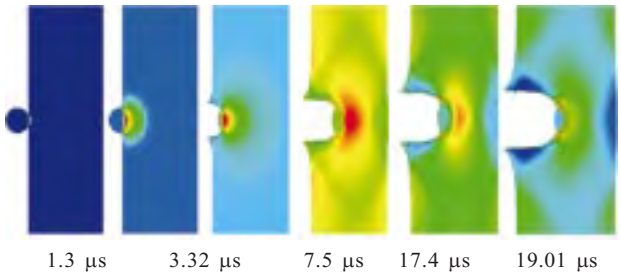

Figure 6. Selected cycle of autodyn simulation showing the impact of a 10 mm dia steel ball impacting mild steel plate at velocity 1888 m/s.

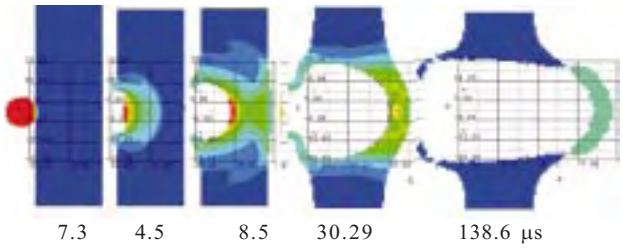

Figure 7. Process of penetration and spalling in 32 mm thick mild steel plate due to impact of a 15 mm dia steel ball at velocity 5264 m/s.

and penetration depth were accurately predicted through simulation. Figure 7 shows the cavity opening and penetration in mild steel plate due to impact of a 15 mm dia steel ball at velocity 5264 m/s. The strain rate is maximum at the time of impact and decreases as the penetration proceeds inside the target, as shown in Fig. 8. Strain rate at the impact point, estimated from autodyn simulation, was found to be 3.5×10^5 s^{-1} for a low velocity ball impact of Fig. 6 and it was up to 1.35×10^6 s^{-1} for a high velocity impact of Fig. 8. In the case of high velocity impact, the simulation

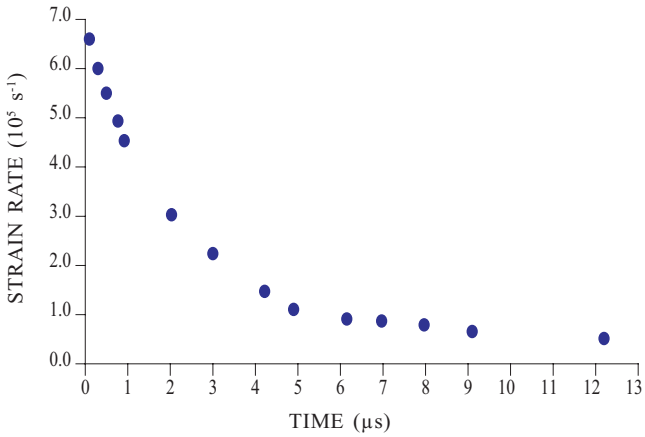

Figure 8. Variation of strain rate with time during penetration in mild steel when impacted by a 7 mm dia ball at velocity 2.4 km/s.

predicts spalling, tensile failure due to the reflection of the initial compressive wave from the rear surface of a finite thickness plate which is common under explosive and intense impact loads. The findings have been validated by the experimental results in terms of hole dia at the front and the rear surfaces of the target plate. Figure 9 shows the comparison between simulated and experimental findings. A 5 mm thick spall and an outer ring from the target plate were actually recovered in the experiment. A minor damage found in experiment to the second air-spaced target plate was due to the impact of spall material from the first plate on to the second plate. Simulations were also performed to map the ejecta of material from the impact surface. Figure 10 shows the flash radiograph of the front surface ejecta versus the simulation results.

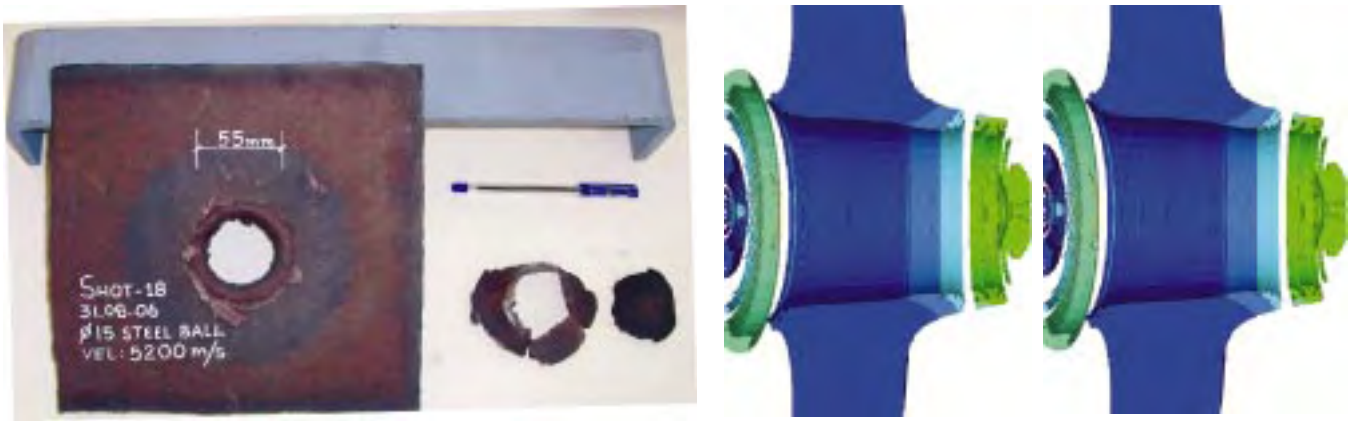

Figure 9. Spall and penetration in target plate: Comparison between experimental and simulation studies.

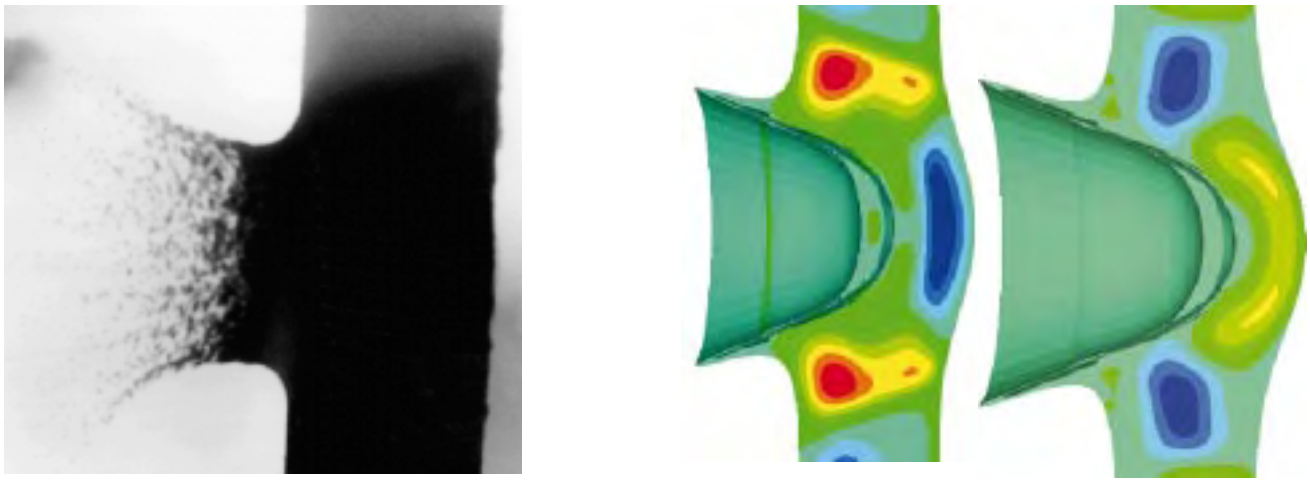

Figure 10. Ejecta of the material from impact surface: Comparison between experiment and simulation.

5. RESULTS AND DISCUSSIONS

The results of crater formed in the target plate due to impact of 7 mm and 10 mm steel balls are given in Table 2. The crater dia at the impact surface and depth of penetration measured in experiments agree well with the predictions through Autodyn simulations. The results show that for a given impactor mass, the ratio of crater dia to depth of penetration decreases with impact velocity. In the two experiments with 15 mm dia ball the target plate was penetrated. The ratio of crater diameter at impact surface to exit surface increases with the impact velocity till it becomes equal.

The dynamic yield strength of mild steel target plate was calculated from Eqn. (17) and is given in Table 3. Impact velocity and crater diameter at impact surface were measured experimentally for this calculations. The dynamic yield strength of mild steel increases from 869 MPa to more than 2000 MPa against the static yield strength of 250 MPa as the impact velocity increases from 1888 m/s to 5264 m/s. This is possibly due to increase in the initial strain rate from 3.5×10^5 s^{-1} to 1.36×10^6 s^{-1} with the increase in the impact velocity. The factor by which the dynamic yield strength of mild steel increases agrees with the previous results[3] of dynamic tensile strengths of aluminium, copper, and mild steel calculated from jet particulation data. The dynamic tensile strength at strain rates of 10^4 s^{-1} to 10^5 s^{-1} was found to be roughly 4-5 times their static strengths.

The dynamic yield strength of steel was also estimated by Kuchner[12] who performed experiments

Table 2. Experimentally determined projectile velocity and crater dimensions formed by the impact of steel ball on to a mild steel target plate.

Exp no.	Projectile (Ball SS-4340)		Velocity, *Vp* (km/s)	Size of crater in mild steel target plate (mm)	
	Diameter (mm)	Mass (g)		Experimental	Simulation
1	10	4.1	1.888	ϕ 20 × 12 deep	ϕ 20 × 12 deep
2	7	1.4	2.400	ϕ15 × 10 deep	ϕ15 × 10 deep
3	10	4.1	3.854	ϕ 30 × 23 deep	ϕ 30 × 22 deep
4	7	1.6	4.786	ϕ 24 × 18 deep	ϕ 24 × 19 deep
5	15	8	3.230	in ϕ 40 – out ϕ 30	in ϕ 40 – out ϕ 24
6	15	8	5.264	in ϕ 55 – out ϕ 55	in ϕ 54 – out ϕ 54

Table 3. Dynamic yield strength of mild steel at different impact velocities calculated using of Eqn (17)

Exp no.	Ball projectile		Velocity *Vp*	Impact strain rate	Target yield strength
	Dia (mm)	Mass (g)	(km/s)	(10^5x s^{-1})	(MPa)
1	7	1.4	2.400	6.4	1223
2	7	1.6	4.786	11.2	1888
3	10	4.1	1.888	3.5	869
4	10	4.1	3.854	11.9	1609
5	15	8	3.230	8.1	1430
6	15	8	5.264	13.5	2010

by impacting 2 mm dia copper jet on steel targets at velocity 7.5 km/s. From the studies on crater volume, he calculated the dynamic yield strength of steel to be 2250 MPa. Experimental data on crater/projectile dia given by references 13 and 14 was used by Szendrei[4] to calculate the dynamic yield strength of steel to be 820-1130 MPa at impact velocity of 3.57 km/s. Figures 9 and 10 show the comparison of all these findings

These studies show that the dynamic strength of target metal is a sensitive function of impact velocity and the strain rate under which the material deforms, thus indicating the strong strain rate sensitivity of mild steel.

ACKNOWLEDGEMENTS

The authors express their sincere thanks to Dr Satish Kumar for his encouragement and kind permission to publish this paper. The authors also express their sincere thanks to Ms Ritu Khurana for putting the paper in the present format, and Mr Manoj Athwal and Mr Girija Nand Jha for their assistance in carrying out the impact experiments using two-stage light gas gun facility.

REFERENCES

1. Follansbee, P.S.; Regazzoni, G. & Kocks, U.F. The transition to drag controlled deformation in copper at high strain rates. *In* Proceedings of Mechanical Properties of Materials at High Strain Rates, edited by J. Harding. Institute of Physics, Conference Series No. 70, London, 1984. pp. 71-80.

2. Milkhailov, A.N. & Trofimov, V.S. Determination of the strength of copper upon dissociation of a cumulative projectile. *Combus., Explos. Shock Waves*, 1979, **15**, 670-74.

3. Singh, Manjit; Bola, M.S. & Prakash, S. Determination of dynamic tensile strength of metals from jet break-up studies. *In* Proceedings of the 19th International Symposium on Ballistics, Interlaken, Switzerland, 7-11 May 2001.

4. Szendel, T. Analytical model of crater formation by projectile impact and in application to calculation of penetration curves and hole profiles. *In* Proceedings of the 7th International Symposium on Ballistics, Den Haag, The Netherlands, 1983. pp. 575-583.

5. Tate, A. A theory for deceleration of long rods after impact. *J. Impact Mech. Phys. Solids*, 1967, **15**, 387-99.

6. Held, M. Determination of the crater radius as a function of time of a shaped charge projectile that penetrates water. *Propell. Explos. Pyrotech.*, 1995, **21**, 64-69.

7. Taylor, G.I. The use of flat-ended projectiles for determining the dynamic yield stress: Theoretical considerations. *Proc. Royal Soc. London*, 1948, **194**(A), 289.

8. Zerilli, F.J. & Armstrong, R.W. Dislocation mechanics-based constitutive relations for material dynamics calculations. *J. Appl. Phy.*, 1987, **61**(5), 1816-825.

9. Kolsky, H. An investigation of the mechanical properties of materials at very high rate of loading. *Proc. Phys. Soc. London*, 1949, **62**, 676-04.

10. Lindholm, U.S. Some experiments with the split Hopkinson pressure bar. *J. Mech. Phys. Solids*, 1964, **12**, 317-35.

11. Karnes, C.H. The plate impact configuration for determining mechanical properties of materials at high rates of strain, edited by U.S. Lindholm. Springer-Verlag, New York, 1968. pp. 270-93.

12. Kuchner, V. Ballistics Research Laboratory Technical Report BRL-TR-ARBRL - TR - 02046. ADA-05 3377, Feb. 1978.

13. Hohlar, V. & Stilp, J. Penetration of steel and high density rods in semi-infinite steel targets. *In* 3rd International Symposium on Ballistics, 1977, Vol. H-3. pp. 1-12.

14. Hohlar, V. & Stilp, J. Influence of the primary yaw angle on the secondary yaw angle during armour plate perforation. *In* 6th International Symposium on Ballistics, 1981. pp. 302-308.

Contributors

Dr Manjit Singh is Scientist F and Head, of both Shock & Detonics Division and Gun Group in Terminal Ballistics Research Laboratory (TBRL), Chandigarh. His areas of specialisation include detonics of high explosives, dynamic shock compression of materials, and high strain rate behaviour of metals. He has published more than 25 papers in national/international journals and conference proceedings. He was deputed to Israel, USA, South Africa, Switzerland, and Germany for presenting his research work in International symposia and conferences. He has received *DRDO Technology Award* in 2001 for his outstanding contributions in detonics and shock dynamics.

Mr Bhupinder Sewak is a Computer Scientist from Madurai Kamaraj University, Tamil Nadu. He is working as Scientist C at TBRL, Chandigarh for the past 17 years. His areas of specialization include modelling and simulation of detonics and shock phenomena. Presently, he is working on the problems of impact and penetration, hypervelocity impact of flyer plate to study EOS of materials under high strain and air blast-induced ground shock, and underground structural damage.

Mr A.C. Sharma is Head, Shock and Detonics Division, TBRL, Chandigarh. He received his Masters from the JK Institute of Applied Physics, Allahabad University. Over his ten years in defence research, he has gained expertise in launching projectiles to very high velocities. His interests include shock and detonics studies, simulation of high strain rate phenomena, impact and penetration, and blast phenomena.

Mr Thomson Mathew is Head, Gun Group, TBRL, Chandigarh. He received his BSc (Mech Engg) from the University of Kerala and Masters from the Thapar University. His expertise includes launching projectiles to very high velocities. His current interests include plate impact experiments, spacecraft shielding from high velocity debris impact, high strain rate studies, and CAD modelling.